

# Evolution of highly-selective gas sensing methods using correlation spectroscopy

J.P. Dakin, Optoelectronics Research Centre,  
University of Southampton,  
SO17 1BJ, UK

## Abstract

This review describes the recent history and latest developments in gas detection at Southampton University, using real-time correlation spectroscopy. The general approach has been to use a gas sample as a matched optical filter, to selectively detect similar absorption spectra of the same gas in a measurement region. All variations of the method exhibit excellent selectivity whenever the gases have narrow line spectra, even when simple broadband sources are used for illumination. Several have been employed in laboratory tests, for remote detection over optical fibre leads. The paper describes work in four main areas. Firstly, our earliest work on a pressure modulation for methane detection is briefly reviewed, secondly a Stark modulation method to form an optical hygrometer is described, thirdly a multi-line light source (formed by combining a broadband optical source with a Michelson interferometer, having a gas cell in one arm) is discussed and, finally the most recent progress with a complementary modulated beam system, using either alternately-chopped or intensity modulated light sources, is described.

## 1. Introduction

Many common gases of industrial and environmental importance exhibit their fundamental optical absorption in the infrared region. Weaker overtone and combinational bands extend into the near infra-red and visible region, hence coinciding with the low loss transmission window for silica fibre. Absorption in these regions is usually due to transitions between vibrational-rotational energy levels of the molecule. As the fine-line structure within an absorption band is highly specific to the gas species, recognition of these features provides for the possibility of highly selective gas detection. The band positions of a selection of common gases are shown in simple form in Figure 1, together with the absorption spectrum of silica optical fibre. Infra-red fibres, typically manufactured from fluoride glasses, are also available with acceptable loss at wavelengths up to 5µm. These latter fibres make the stronger fundamental gas absorptions also accessible via remote leads, thereby enhancing the potential detection sensitivity, but have a much higher cost and are not so mechanically robust.

The low loss of silica optical fibres allows a gas sampling cell to be located many kilometres from the monitoring station with little degradation of the signal, and the rugged nature and continually-reducing cost of fibre cables makes this an ever more attractive option. The passive nature of the sensor head, and the low optical power used, makes such optical techniques inherently safe for hazardous applications, such as the monitoring of explosive gases<sup>1,2</sup>.

Early fibre-optic based methods measured gas transmission using broadband LED sources<sup>3</sup> and thus had poor selectivity. Other recent methods have used laser sources<sup>4</sup>, but these can present problems due to their long coherence length; in particular modal noise effects (ie.. "laser speckle"-type effects) in multimode fibre. Even when single mode fibre is used to prevent this, effects such as unintentional Fabry-Perot etalons between fibre ends in connectors, and more complex interference patterns within the measurement cell and launch optics, can potentially cause severe practical limitations. Trace-gas sensors often operate with very low absorption levels, so minor perturbations due to interference effects can be severe.

Correlation spectroscopy<sup>5,6,7,8</sup> allows the use of a broadband source, yet still monitors the fine

spectral features of the gas spectrum. It has the further advantage of employing all of the spectral information contained in the selected gas absorption band, rather than just a single line, thereby enhancing the cognitive nature of the technique.

Our basic methods of real-time correlation spectrometry all involve modulation of the absorption spectrum of the reference gas sample, relative to the gas to be measured. Modulation can be achieved directly by varying the absorption spectrum of the reference gas. In an earlier paper<sup>3</sup>, we reviewed progress with three modulation techniques, each using the correlation spectroscopy method. These included Stark and pressure modulation of the gas sample and phase modulation of light travelling between samples. In essence, a common optical configuration was adopted for all of the schemes investigated in the study, as shown schematically in Figures 2(a) and 2(b). The apparatus comprised two gas cells, through which light from a broadband source was passed sequentially, prior to detection. In the fibre-remoted version, light was conveyed to the cells via multimode optical fibre, and a bandpass filter was included before the detector in order to attenuate any extraneous light lying outside the absorption band manifold of the relevant gas. The gas to be detected was directed into the measurement cell, whereas the reference cell was filled with a known concentration of the gas to be detected and then sealed.

Modulation of the absorption spectrum of either gas cell resulted in a change in the correlation between the transmission spectrum of the measurement gas sample and the reference gas, thereby causing a variation in the total transmission of the system. The absorption spectrum of the gas contained in the reference cell was modulated, either directly or indirectly, in order to produce the desired signal. The synchronously-detected output signal then depended on the concentration of the correlating gas in the measurement cell.

Modulation methods which act directly on the gas include Stark and pressure modulation, as depicted in Figure 2(a). The pressure modulation technique is applicable to all gases with appropriate absorption, but is most selective with simple gases having narrow line spectra. It involves periodically pressurising the gas within the reference cell, causing a variation in both the strength and width of the absorption lines. Stark modulation of gases occurs only with polar molecules and results from the splitting (or, at atmospheric pressure the broadening) of individual absorption lines when a large electric field is applied.

Our third modulation approach is indirect and involves a redistribution of the optical spectrum of the light, as it passes from the measurement to the reference cell, as shown schematically in Figure 2(b). Angle modulation of the light (using phase or frequency modulation), which alters the spectrum of light before passage through the second cell, is a means of achieving this.

The final approach discussed differs in architecture from that in fig 2, in that two sources are used with complementary modulation (ie. 180 degrees phase difference) of their intensities, and one of these is passed through a (reference) gas cell before the beams are recombined. The intensities of the beams are adjusted so that this combined beam has no net modulation, and it is then used as a probe beam for detection of the same gas as that in the reference cell. If the same gas is present in the measurement region, a net modulation is then observed.

All these methods will be discussed in more detail below.

## **2. Brief review of early work on methane detection using pressure modulation spectroscopy.**

Our early work on methane detection<sup>7</sup> used a pressure modulation cell formed from a cylindrical rod with an axial, cylindrical hole, bored part way into it, to contain the gas. One end therefore terminated in the metal end-wall, whereas the other end was sealed by a thin piezo-electric (PZT on a thin metal base) diaphragm, of a type commonly used in alarm clocks. The light entered and left through glass windows in the wall of the cylinder, and the light path was across a diagonal of the cylinder close to the metal end wall, ie. across the region of maximum pressure variation when the methane gas

content of the cylindrical hole was driven into acoustic ("organ-pipe") resonance using the PZT. This formed the reference cell of fig 2. The measurement cell was a multi-pass White cell of 4.8m pathlength, and the transmitted light was detected using a PIN detector and transimpedance amplifier, followed by a simple lock-in amplifier referenced to the PZT drive signal. Using this arrangement a noise-limited measurement resolution of 50ppm methane was achieved. More details of this method were given in ref 7.

### 3. Water vapour sensing (hygrometry) using Stark-modulation spectroscopy

In our earlier paper<sup>8</sup>, Stark Modulation was used for the detection of ammonia gas. The Stark effect is potentially very attractive, as it is only necessary to apply an electric field to the gas cell in order to cause a synchronous modulation of the detected signal. The only disadvantages are the high field strength required to produce even a low amplitude modulation index in the detected signal and the fact that only certain gases are Stark-active. In order to be Stark-active (i.e. suffer line splitting or broadening under the influence of electric field) a gas must have a strong electrical dipole moment. Traditional water vapour sensors have many applications in industry and meteorology. Despite many different types having been commercially available for many years, there are few, if any, hygrometers which perform reliably over an extended temperature range.

The H<sub>2</sub>O molecule is strongly polarised and therefore has the necessary dipole moment for Stark modulation. However, as water is not particularly volatile at room temperature, a heated Stark cell is necessary, firstly to maintain a sufficiently high vapour pressure in the cell to produce a strong absorption and secondly to prevent the possibility of condensation on the windows or electrical components, which would occur if the cell were to cool below the dew point.

The basic design of our prototype cell<sup>9</sup> is shown in Figure 3. The 160 mm x 18 mm x 5 mm electrodes were held 6 mm apart using polymer spacers. The electrode/spacer structure was mounted in a horizontal glass tube fitted with end windows. The horizontal tube (the reference gas cell) was connected to a lower-level water reservoir. Both gas cell and water reservoir could be heated electrically, with the reservoir being held at the lower temperature. The gas cell was connected to an electrical drive unit, via feed-through leads sealed into the glass walls, in order to provide a high field strength across the water vapour between the electrodes.

The electrical drive to the Stark cell was applied using a combined, AC + DC, high voltage unit, capable of applying a 2.0 kV p-p AC signal at 7.1 kHz with a 2.0 kV DC bias signal. The latter was necessary to ensure the Stark modulation component occurred at the fundamental frequency of 7.1 kHz rather than twice this, as Stark modulation of the optical amplitude is approximately proportional to the square of the applied voltage. The Stark effect results in a modulation of the linewidth of the gas absorption in the reference cell, which changes the effective overlap integral of the gas absorption in the reference cell, and that of the measurement one<sup>8</sup>.

In order to detect the small AC modulation signal at the detector, the lock-in amplifier arrangement shown in Figure 4 was used. In order to determine the modulation index of the received light, and hence reference the detection scheme, a DC signal was also derived from the output of the transimpedance receiver.

Figure 5(a) shows the detected signal when light from a tungsten halogen source was collimated through the Stark cell and detected via a narrow band interference filter corresponding to the water band  $1.94 \mu\text{m} \pm 10 \text{ nm}$ . The two states represent conditions when the beam was allowed to reach the detector and when the beam was blocked off. Using a monochromator, it was confirmed that the modulation only occurred in the main water bands at  $1.4 \mu\text{m}$  and  $1.9 \mu\text{m}$ .

The optical modulation arises from the change in the (pressure-broadened) width of the absorption lines under the action of the electric field in the reference cell (Stark cell). When the absorption lines are strong (ie. close to 100%) this leads to a change in the optical loss in the cell. The water vapour content of the laboratory air was monitored in a 35 cm long measurement cell, in line with

the reference cell. In order to check the signal change due to the H<sub>2</sub>O absorption in this path, it was alternatively filled with air containing water vapour at a partial pressure of approximately 12 mbar and with dry nitrogen. The resulting change in detected signal has so far been very weak, but it is nonetheless discernable and reproducible, and it represents the first detection of water vapour by this method (see Fig 5(b)).

It should be noted that our gas sensing result using this novel arrangement is a preliminary one and steps are being taken to improve our signal to noise ratio for quantitative detection of water vapour. One attraction of the Stark method is that it is compatible with the use of long-term averaging to improve the signal/noise ratio.

We shall now describe the second area of progress, that of our new light source arrangement.

## 4. Novel multi-line source for gas sensors, using a Michelson Interferometer.

### 4.1. Basic description

Our new light source relies on the condition of destructive interference which it is possible to establish in a suitably-aligned Michelson Interferometer (see Figure 6). This condition occurs when the interferometer is set up with a path length difference of  $\lambda/2$  between the two arms. Then, provided the reflected powers are equal, and provided the mirrors and beam splitters are suitably flat, the optical signals in the appropriate output port will destructively interfere. The cancellation is effective over a fairly wide optical bandwidth, usually much wider than a typical ro-vibrational absorption-band manifold of a gas. If a gas, of the type to be detected, is now introduced into one arm of the interferometer, the light in that arm will be selectively attenuated, at all the lines in the gaseous absorption manifold. Light returning from the other (gas-free) arm, at these particular wavelengths, is then no longer effectively cancelled, as there is now insufficient energy returning from the gas-filled arm to interfere with it in a totally destructive manner. As a result, the energy from the output port will consist of a series of narrow discrete spectral lines, having significant power only in the wavelength regions where the gaseous absorption is significant.

Our new source is highly attractive for gas sensing, as it is certain to be well matched to all of the significant gaseous absorption lines of the gas to be detected. The contrast of a gas sensor can be greatly improved using such a source, as it contains negligible energy at wavelengths where there is no gaseous absorption and has maximum energy at the strongest absorption peaks. Secondly, because, unlike a conventional broadband source, there is a no "wasted" optical energy in the spectral regions between the absorption lines, problems due to excess photon noise in the optical receiver, are minimised. Thirdly, unlike a single discrete laser line, the multi-line source is less likely to suffer from undesirable coherence effects. Such problems can occur with laser sources whenever there is specularly reflected light from the windows of a gas measurement cell, or when there is intermodal interference in a multimode optical fibre cable.

### 4.2. Theory of the Michelson Source

The Michelson interferometer (Figure 1) has an output power  $P_{OUT}$ , given by where  $P_0$  is a constant,  $k$  is the fringe contrast,  $\Delta L$  is the total effective path difference between interfering beams and  $\lambda$  is the optical wavelength.

$$P_{OUT} = P_0 \left[ 1 + \cos \left( \frac{2\pi \Delta L}{\lambda} \right) \right] \quad (1)$$

If the Michelson interferometer exhibits perfect cancellation, at the nulls (ie..  $k = 1$ ), then:-

$$P_{OUT} = P_O \left[ 1 + k \cos \left( \frac{2\pi \Delta L}{\lambda} \right) \right] \quad (2)$$

and there is a null when  $\Delta L = \lambda/2 \pm n\lambda$ .

Close to the condition  $\Delta L = \lambda/2$ , (ie. when  $n = 0$ ), cancellation at a null is effective over a relatively broad bandwidth, due to the slowly changing nature of the cosine function near its maxima and minima. It is useful to illustrate this with a numerical example: If the interferometer remains fixed, but the wavelength of the input light changes from the perfect central-wavelength "null" condition by only 3%, there will be a tiny uncanceled power output at this new wavelength equivalent to only 0.0044% of the peak output,  $2P_O$  (ie., that which would occur under conditions of constructive interference).

Alternatively, if, at a particular wavelength, the light in one arm is totally attenuated due to gaseous absorption, all of the light returning from the other arm at that wavelength (except for the inevitable 3dB loss in the beam combiner) will contribute to the output.

There are two additional theoretical factors to consider in the analysis of our Michelson interferometer when gas is present in one arm. Firstly, the finite refractive index of the gas, compared to normal air, causes a small phase imbalance in the system, requiring a small change in the length of this arm in order to set it to  $\lambda/2$  total path difference. Secondly, it is necessary to consider the effect of anomalous dispersion, ie.. the more dramatic change in refractive index with wavelength which occurs in the region close to an absorption line. It should be noted, of course, that anomalous dispersion could either be unimportant, a disadvantage, or even an advantage depending on its magnitude. Clearly, if it only occurs to a significant degree when the absorption is close to 100%, its effects will not be significant, as a phase change in a very weak transmitted signal will not affect the operation of our source. However, if the total (2-way) phase shift due to anomalous dispersion were to be a substantial fraction of  $180^\circ$  (ie.. a substantial fraction of the desired total path difference of  $\lambda/2$  in our interferometer), then this phase shift could be utilised, instead of the gas absorption, to give a line-spectrum output at selected wavelengths.

In order to calculate the effects of anomalous dispersion, we shall examine the behaviour of plane wave propagation in an absorptive medium.

- The electric field  $E$  of a propagating plane wave is given by:-

$$E = E_0 e^{i(kx - \omega t)} \quad (3)$$

where  $x$  is distance,  $\omega$  = angular frequency and  $t$  = time.

The wavenumber,  $k$ , represents the number of complete  $2\pi$  phase changes which occurs, per unit length of propagation, and is given by:-

$$k = \beta + \frac{i\alpha}{2} \quad (4)$$

where  $\beta$  is the real component of the wavenumber (this represents the phase-change coefficient in a lossless medium) and  $\alpha/2$  is the imaginary component. The quantity  $\alpha$  is the attenuation coefficient, usually expressed in  $\text{cm}^{-1}$ . (The factor of 2 arises because  $\alpha$  is the *power* attenuation coefficient, whereas the equations above represent electric field).

The modulus of  $k$  is given by  $\left(\beta^2 + \frac{\alpha^2}{4}\right)^{1/2}$  and the perturbation, due to absorption, of the phase change in the gas-containing arm in our interferometer then becomes significant when the quantity  $2L[(\beta^2 + \alpha^2/4)^{1/2} - \beta]$  becomes a significant fraction of  $\pi$ , (i.e. the additional phase change due to absorption approaches  $180^\circ$ ). The anomalous dispersion therefore only becomes significant under conditions of very high absorption. Under such conditions, the light in the gas containing arm will be effectively absorbed so its phase will be irrelevant. We can therefore confidently ignore anomalous dispersion.

### 4.3. Experimental results with the Michelson source

The source was tested using the arrangement shown in Figure 3. The Michelson arrangement was set up using an Ealing optics "Universal Interferometer" unit, fitted with  $\lambda/4$  mirrors and  $\lambda/10$  beamsplitter. Clearly, components of better quality are desirable for best fringe contrast, but this was useful for the first experimental verification of our new source. With the interferometer set to give maximum fringe contrast (i.e. close to equal path condition) the length of one arm was adjusted to minimise the signal from the output port (i.e. set up the condition of destructive interference). Under these conditions, a series of discrete spectral lines were clearly visible on the display of the Ando spectrometer unit (see Figure 7(a)). When the path length was adjusted for constructive interference at the output port, then a broadband light output was obtained, with dips in intensity where the methane gas has absorbed energy (see Figure 7(b)).

## 5. Complementary-modulated-beam approaches to correlation spectroscopy

### 5.1. Introduction to complementary-modulated-beam methods

Another approach to modulation spectroscopy avoids the need to modulate the optical properties of the reference gas by periodically switching between two light paths, one passing through and one bypassing the reference cell, before passing through the gas measurement cell. We present two different arrangements by which the light intensity in each path may be modulated. One path is arranged in free space, and sees no spectral filtering, whereas the other path contains a cell filled with the reference gas. For convenience, the system uses two separate white light sources. This has the advantage that the light intensity of each can be independently adjusted to balance the intensities, merely by changing the supply voltage. After collimation, one beam is directed through the reference cell, before joining the second collimated beam in a beam combiner. The united beams (now co-linear), are directed through the measurement cell, a filter (in our case, a monochromator) to select the gas band, and are finally incident on the detector.

Our first method is implemented using a chopper wheel, to alternately block one light path and then the other. Before entering the combiner, both beams pass through the plane of the chopper wheel, where they are alternately blocked. With the reference cell filled with the reference gas, and the monochromator set to the correct wavelength, the relative intensity in each channel was adjusted with no gas in the measurement region. This was set to the condition where the difference in detected signals was essentially cancelled. After this initial setup-procedure, to "zero" the system without gas, the measurement cell was alternately filled with sample gas and dry inert gas to demonstrate operation of the system.

It is clear that the two temporally-diplexed (i.e. time-interleaved) beam components have similar total intensity, the only difference being that one component has less energy in the narrow-spectral regions corresponding to the gas absorption lines. Thus, if the two beams pass through a medium with a flat spectral absorption, their intensities will remain the same. If, however, they pass through a gas with similar absorption bands, the component which did not initially pass through the reference cell will be more heavily attenuated (as it initially has more light energy present in the regions corresponding to the absorption lines of the gas).

Our second approach is similar, except that we intensity modulate the light sources themselves, thereby avoiding the need for moving parts (i.e. the chopper wheel). The light sources are modulated with oppositely polarised signals, the sinusoidal modulation waveform being generated by a custom-made generator, providing complementary sine wave modulation signals, with a relative phase shift of  $180^\circ$ . Each of the two components from the sine wave generator is used to drive a separate lamp, in combination with a D.C. bias. The two beams are combined, as before, and used to interrogate gas in the measurement cell. We shall now describe the experimental system in more detail.

## 5.2. Experimental Arrangement

### 5.2.1. Correlation gas sensor driven by alternately-chopped free-path and reference beams

Figure 8 shows the experimental setup used for the alternately-chopped path-modulation arrangement. Two separate quartz halogen lamps (6 V, 10 W) were used as light sources. The light intensity of each was independently adjustable by changing the D.C. supply voltage to each. Collimated beams were formed using silica lenses ( $f=50$  mm). One beam was directed through the reference cell (pathlength was 180 mm, and the cell used silica windows), and a fraction of this was redirected to combine co-linearly with a fraction of the second beam, using a standard cube-type beam combiner. This had a nominal 50:50 (i.e. 3dB) power ratio. As described above, both beams passed through the plane of the chopper wheel, where they were alternately blocked, before reaching the combiner. The united beams passed on through the measurement cell (this had a path length of 300 mm and also had silica windows), the monochromator to select the gas absorption band, and then on to the GaInAs-photodiode detector. The latter had a responsivity of approximately 0.3 A/W between 1.5  $\mu\text{m}$  and 2.0  $\mu\text{m}$ . The detected signal was measured with a phase-independent lock-in amplifier (Stanford Instruments), synchronized to the chopping frequency. From measurements of the detected signal, and using the data sheet value for the responsivity of the detector, the mean detected optical power was calculated to be approximately 6.6 nW and 2.6 nW, at the principal measurement wavelength of 1.505  $\mu\text{m}$  and 1.92  $\mu\text{m}$  respectively. Before introducing a gas sample into the measurement cell, the relative intensity in each beam was adjusted such that the detected lock-in signals, with no gas present in the sample cell, was minimized. (*Note:* The relative intensity adjustment had to be repeated, when the wavelength was changed). After this initial setup-procedure to "zero" the system without gas in the measurement cell, this cell was alternately filled with a test sample of gas (ammonia plus water vapour was used in our first tests) and swept with a dry inert gas (nitrogen).

For our first measurements, the reference-cell and measurement gas samples were generated by half-filling a large flask with a concentrated ammonia solution in water. The head space of the flask therefore contained a mixture of water vapour, ammonia gas, along with, after partial evacuation using a vacuum pump, a negligible fraction of residual air. This  $\text{NH}_3$ -water vapour mixture was then present at a total pressure of 1 Bar and at room temperature. The saturated partial pressure of water vapour in the head space was estimated to be roughly 20 torr, at this temperature and hence the partial pressure of ammonia was estimated to be around 740 torr. To fill the gas cells, further gas was drawn out from the head space in the flask, allowing time for more ammonia and water vapour to escape from the solution.

This gas mixture allowed testing of the system using either water vapour or ammonia, depending on which wavelength band we selected with our monochromator filter. The monochromator was set to  $\lambda=1.92$   $\mu\text{m}$  for water vapour measurements, and to  $\lambda=1.505$   $\mu\text{m}$  for measuring the concentration of ammonia vapour. (The monochromator bandwidth was 20 nm).

### 5.2.2. Correlation spectroscopy using complementary (opposite-polarity) intensity modulation of light sources

We shall now describe more details of the experimental arrangement for the complementary modulated-source methods discussed above. The measurement arrangement is shown in Figure 9. In

this system, the two halogen lamps (again 6 V, 10 W) were connected to a custom-made power source providing two complementary sine wave outputs, which had a phase shift of 180° to each other, in addition to providing D.C. bias for each. The intensity of each lamp was independently adjustable by changing the relative voltage of each power supply. Figure 10 shows the drive signal to each lamp.

As with the chopped-beam system, the detected signal was again fed into a phase-independent lock-in amplifier, in this case synchronised to one of the complementary sine-wave drive signals to the lamps. As before, the relative intensity in each channel was initially adjusted to minimise the detected lock-in signal, with no gas present in the measurement cell.

Similarly, for the gas detection tests, the reference cell was filled with ~740 torr ammonia, and ~20 torr water vapour, at 25°C and atmospheric pressure and the same absorption lines 1.92 μm (water vapour) and 1.505 μm (ammonia) were monitored.

### **5.2.3. Independent measurement of NIR spectrum of the gas mixture used in the measurement and reference cells**

To confirm our choice of measurement bands for water vapour and ammonia, a near-IR transmission spectrum of our experimentally-used gas mixture was recorded with a Perkin-Elmer FTIR spectrometer (see Figure 11). This was measured in a slightly shorter gas cell, having a path length of 160 mm, to fit into the instrument.

### **5.2.4. Results with our complementary modulated beam gas sensor**

Both the chopped-beam system and the modulated-light-source system described above were tested. In each case, results were obtained for the detection of the presence of water vapour and of ammonia gas. The correlation signal was recorded consecutively at three different wavelengths; 1.505 μm, 1.92 μm, and 1.42 μm. The latter wavelength was used to verify the correct origin of the correlation signal, as the absorptions of both H<sub>2</sub>O vapour and NH<sub>3</sub> gas are insignificant at this wavelength (see Figure 11). Figure 12 shows the difference in signal, when the measurement cell was alternatively filled with sample gas (NH<sub>3</sub> + water vapour), and pure nitrogen, respectively, each gas mixture being at atmospheric pressure and room temperature. The signals were recorded with a lock-in integration time of 100 ms, in order to demonstrate the potential for fast response times of our gas sensor. The two curves correspond to water-vapour (1.92 μm) and ammonia vapour (1.505 μm) absorptions, depending on the wavelength range selected. Figure 13 shows an overlay of similar measurements at the same three wavelengths (1.55 μm, 1.92 μm and 1.42 μm), again with the cell alternatively filled with sample gas, and pure nitrogen, but in this case the measurement was performed using the modulated-light-source method. It was found that the signal/noise was better for the latter system. (It is probable that mechanical vibration may have generated additional noise in the chopper-based system).

## **6. Conclusions**

We have reported the first measurements of water vapour concentration using Stark modulation of a reference cell and have described a novel light source for gas sensing applications. We propose in future to build an improved version with more rugged construction for use as a source for gas sensing. This should enable us to use a broadband source for gas sensing, yet achieve high contrast measurement. We also hope to report on gas measurements using our novel source at a later date. We have also described new results with two simple configurations for complementary-beam correlation spectroscopy. It is clear from our results that these methods work well in practice, despite their simplicity.

## **Acknowledgements**

The author would like to give particular thanks to Dr H.O. Edwards for the early experimental work on correlation spectroscopy<sup>7,8</sup> and the Michelson source and Dr B.H. Weigl who was primarily involved with the experimental work on the water vapour sensor and the complementary-modulated



beam systems. The author would like to thank Shell Research, Thornton for supporting initial feasibility studies on the Stark cell for water vapour detection and also wish to thank Dr Paul Morkel for his valuable discussions and novel ideas on the Michelson source.

## References

1. P.C. Hills, P.J. Samson and I. Webster, "Explosion hazards of optical fibres in combustible environments", *Proceedings 7<sup>th</sup> Optical Fibre Sensors Conference, Sydney*, (1990) p.63.
2. N.P. Ludlam, "Safety of optical systems in flammable atmospheres", Report for Optical Sensors Collaborative Association, U.K., (R/1008/00/A), 1989.
3. A. Hordvik, A. Berg and D. Thingbo, "A fibre optic gas detection system", *Proceedings 9<sup>th</sup> European Conference on Optical Communications*, (1983) p.317.
4. T. Kobayasi, M. Hirana and H. Inaba, "Remote monitoring of NO<sub>2</sub> molecules by differential absorption using optical fibre link", *Applied Optics*, vol.20, (1981) p.3279.
5. R. Goody, "Cross-correlating spectrometer", *Journal of the Optical Society of America*, vol.58, (1968) p.900.
6. F.W. Taylor, J.T. Houghton, G.D. Peskett, C.D. Rogers and E.J. Williamson, "Radiometer for remote sounding of the upper atmosphere", *Applied Optics*, vol.11, (1972) p.135.
7. H.O. Edwards and J.P. Dakin, "A novel optical fibre gas sensor employing pressure-modulation spectrometry", *7<sup>th</sup> Optical Fibre Sensors Conference, Sydney, Australia*, (1990), p.55.
8. J.P. Dakin, and H.O. Edwards, "Gas sensors using correlation spectroscopy, compatible with fibre optic operation", *Sensors and Actuators B, (Chemical Sensors)*, vol.11, (1993) pp.9-19.
9. J.P. Dakin, H.O. Edwards, B.H. Weigl, "Progress with gas sensors using correlation spectroscopy", *Sensors and Actuators B (Chemical Sensors)*, vol.29, (1995) (To be published).

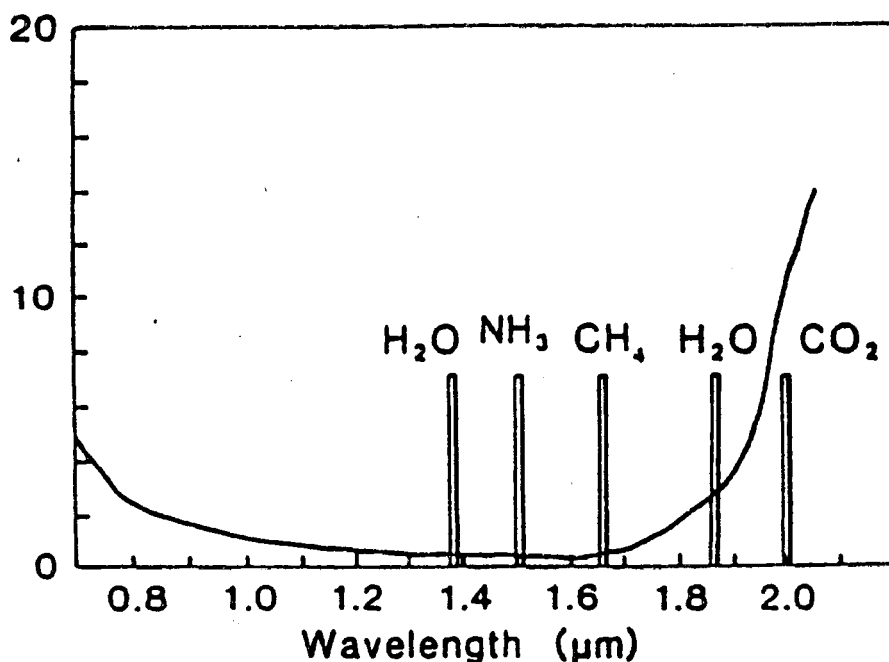
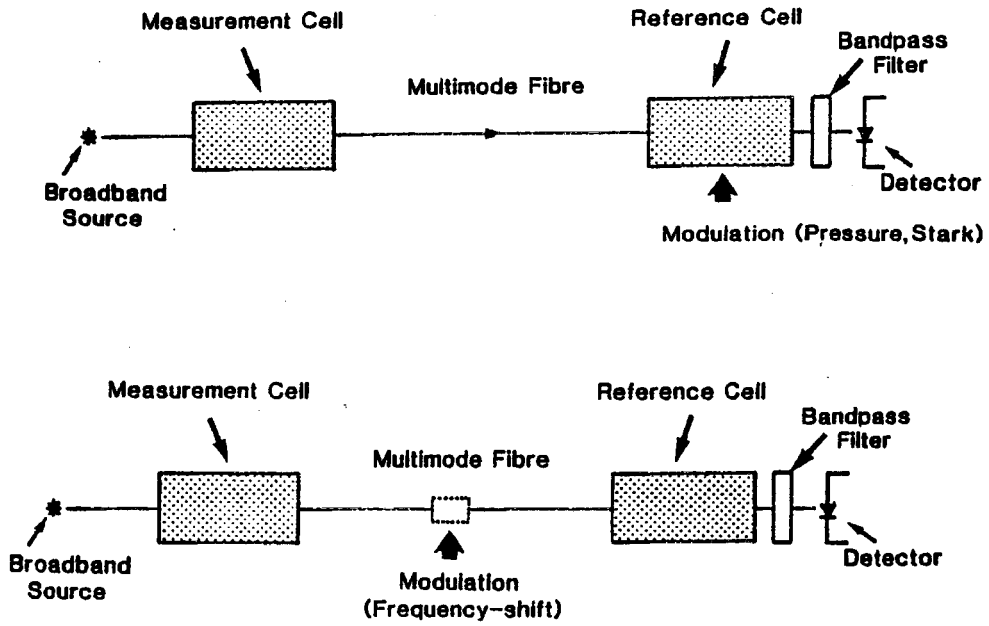
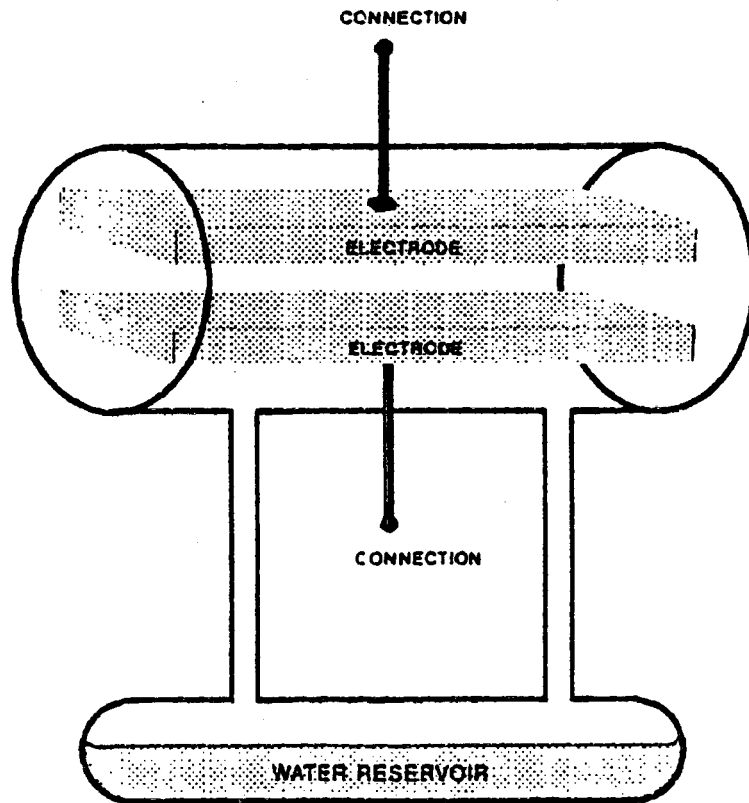


Figure 1 : Absorption bands of some common gases within the transmission window for silica fibre



**Figure 2 : Schematic diagram of correlation spectroscopy concept  
 (a) pressure and Stark modulation, and (b) angle modulation between cells**



**Figure 3 : Schematic of experimental Stark cell for applying electric field to a water vapour sample. (Upper cell is heated above temperature of lower cell to avoid condensation).**

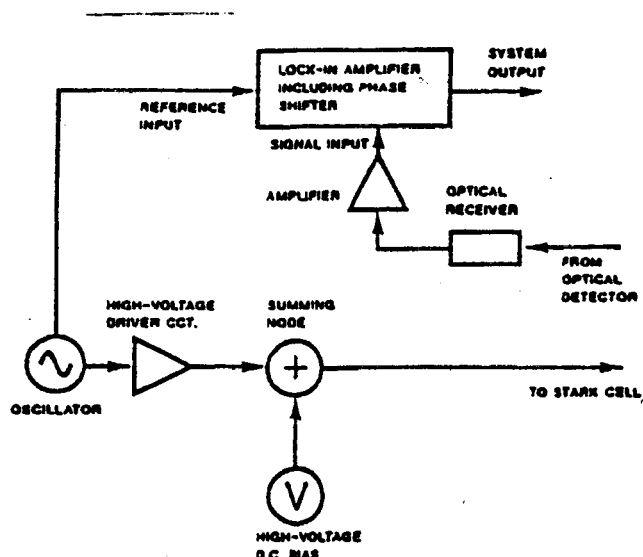


**Figure 4 :** Functional block diagram of electronic system for driving the Stark cell and detecting the modulation signal from the transmitted light.

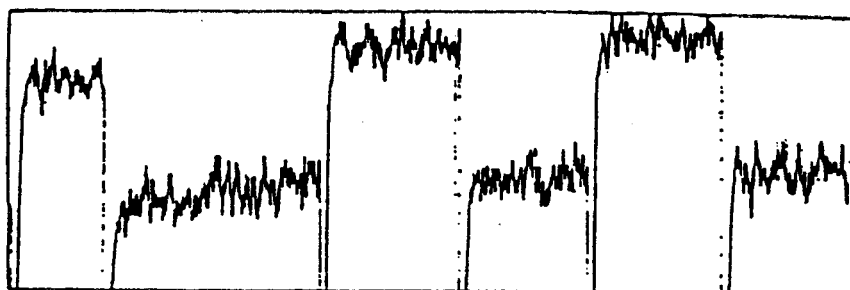


**Figure 5(a) :** Detected signal transmitted through the Stark Cell after phase-sensitive detection using the arrangement of Figure 4. The curve shows the signal change when the light beam is periodically blocked by a shutter. This modulation is only observable in the main H<sub>2</sub>O absorption bands at 1.4  $\mu\text{m}$  and 1.9  $\mu\text{m}$ .

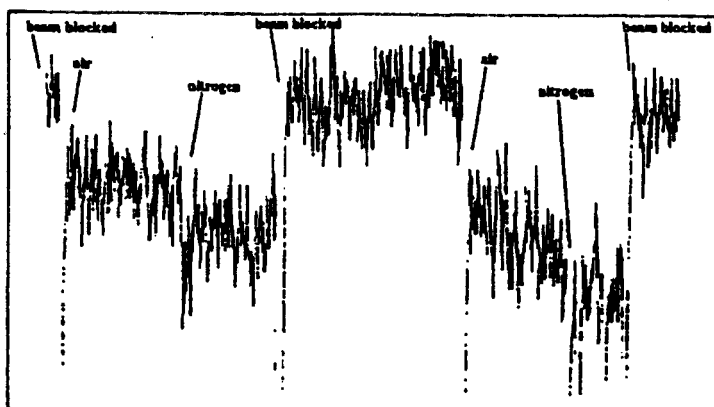


**Figure 5(b) :** Signal change due to H<sub>2</sub>O absorption in the measurement cell. The cell was alternatively filled with air (containing 12 mbar H<sub>2</sub>O-vapour) and dry nitrogen. After each cycle, the beam from the tungsten halogen source was blocked.

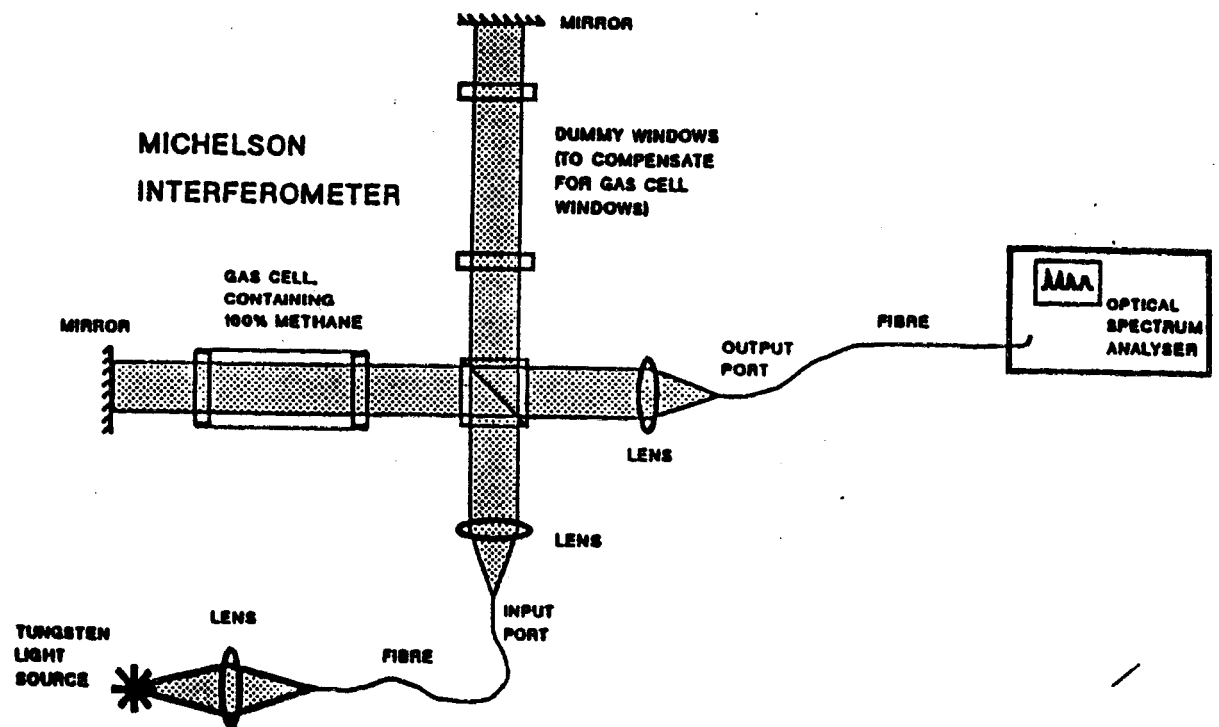


**Figure 6 : Testing arrangement for the novel light source arrangement. The output of the source was connected to an optical spectrum analyzer via an optical fibre lead.**

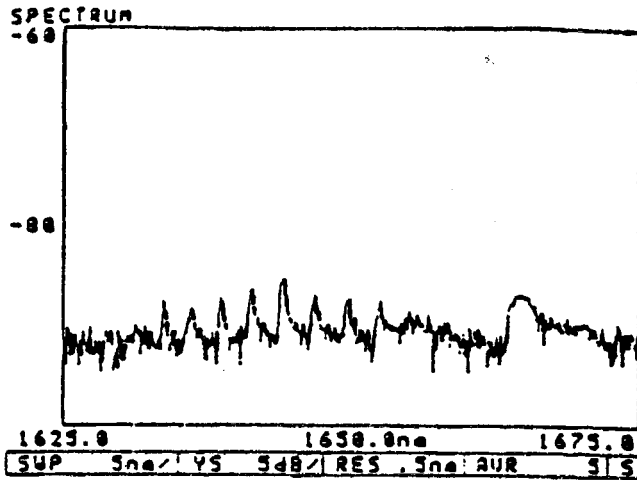


Figure 7(a) : Output (log scale) of Michelson Interferometer with path lengths set to minimise power from output port. The output is maximum at wavelengths corresponding to methane absorption lines, with a low level background signal between these lines.

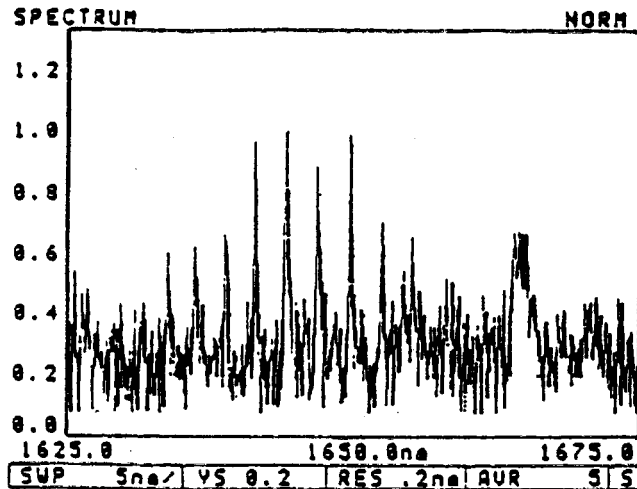


Figure 7(b) : Output (linear scale) of Michelson Interferometer with path lengths set to minimise power from output port. The output is maximum at wavelengths corresponding to methane absorption lines, with a low level background signal between these lines.

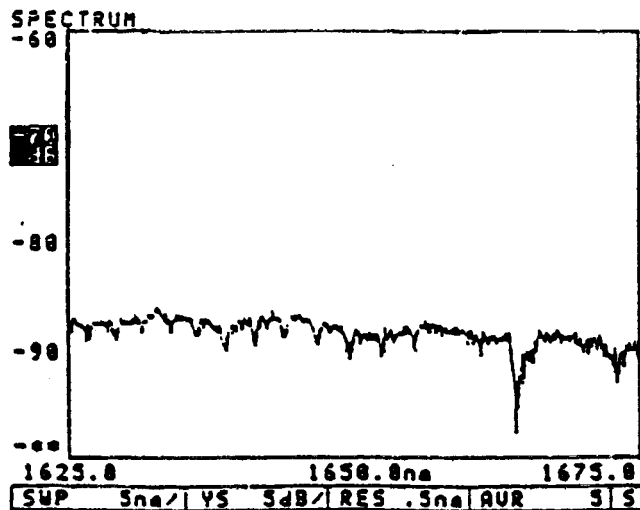
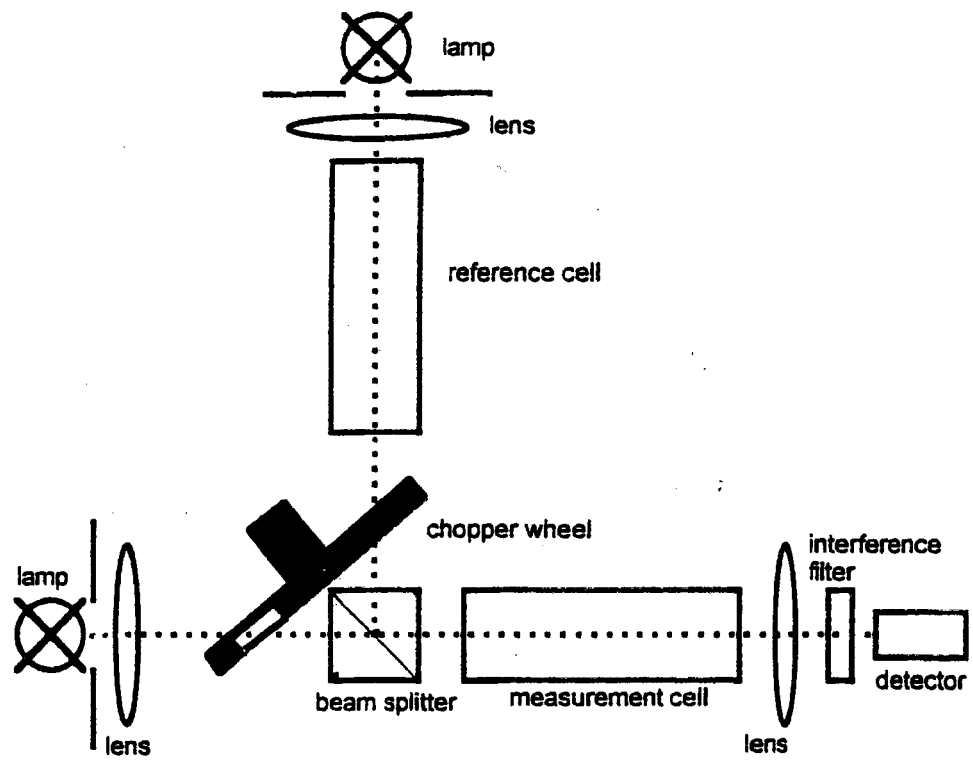
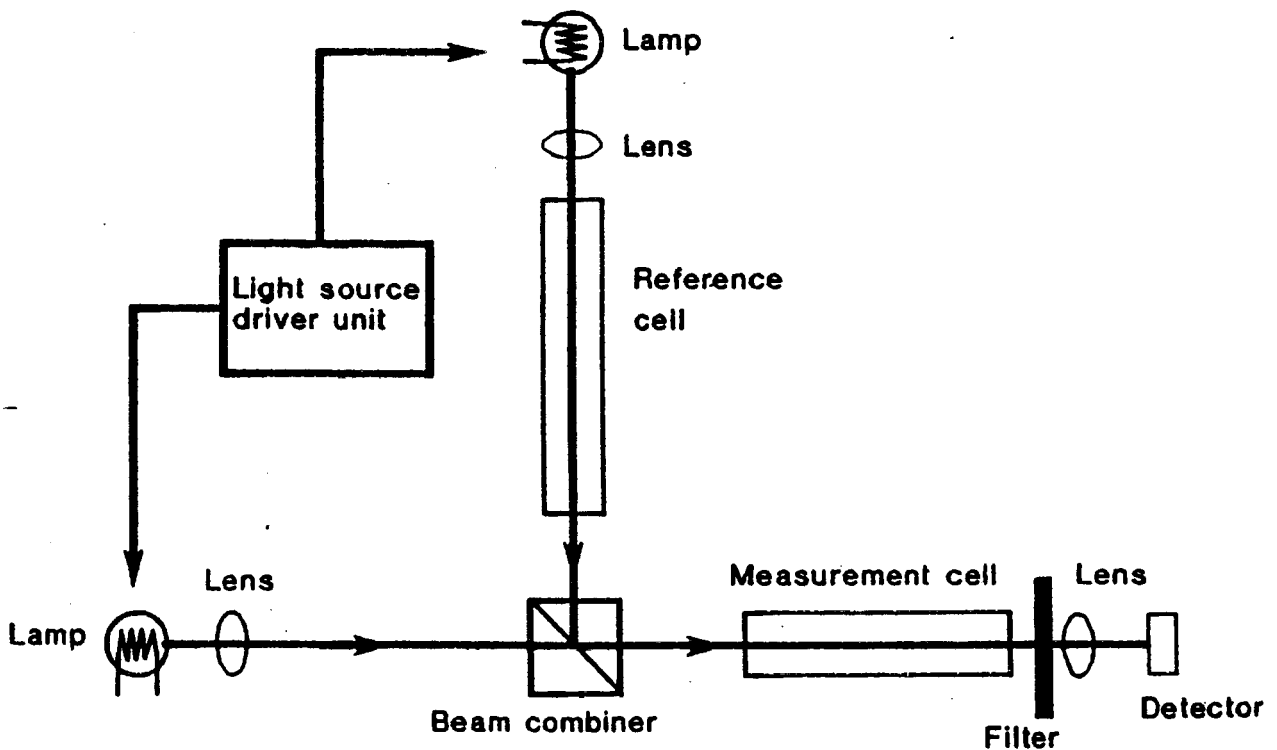


Figure 7(c) : Output (log scale) of Michelson Interferometer with path length set for maximum signal from output port. The output has "dips" corresponding to methane absorption lines.



**Figure 8 : Schematic diagram of the alternately-chopped-path correlation spectroscopy scheme.**



**Figure 9 : Correlation-spectroscopy arrangement using complementary-modulated sources.**

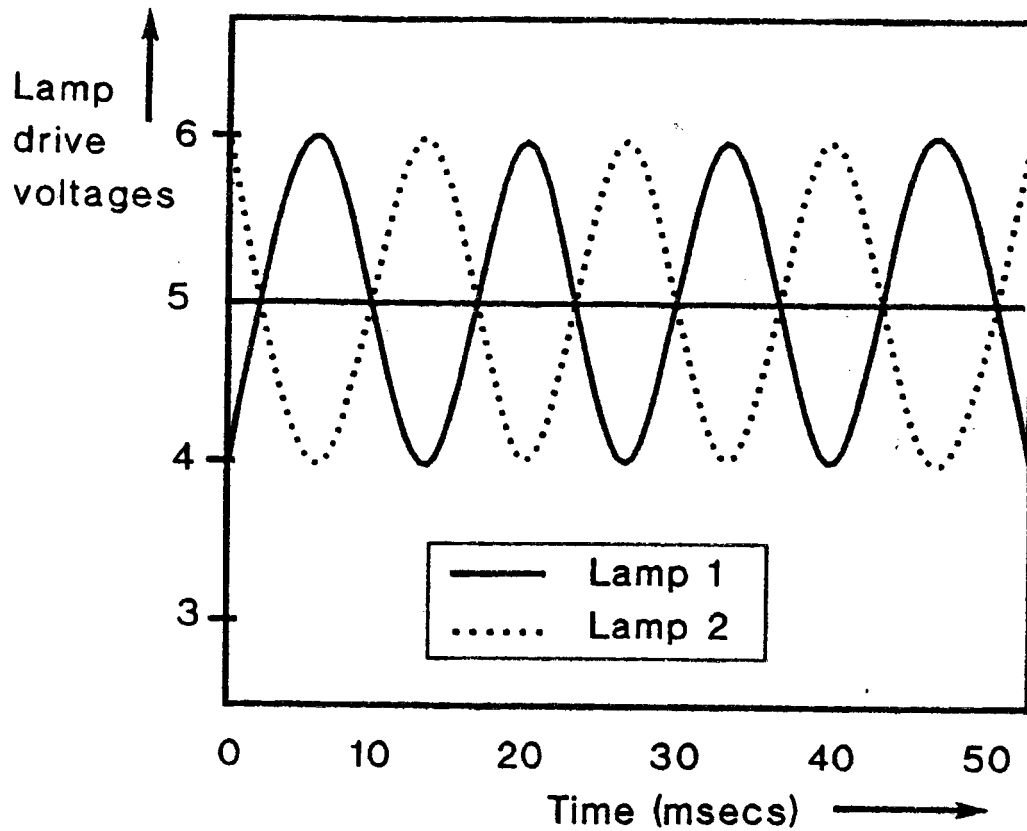


Figure 10 : Sine modulated lamp voltage for each lamp, with arrangement in fig 9.

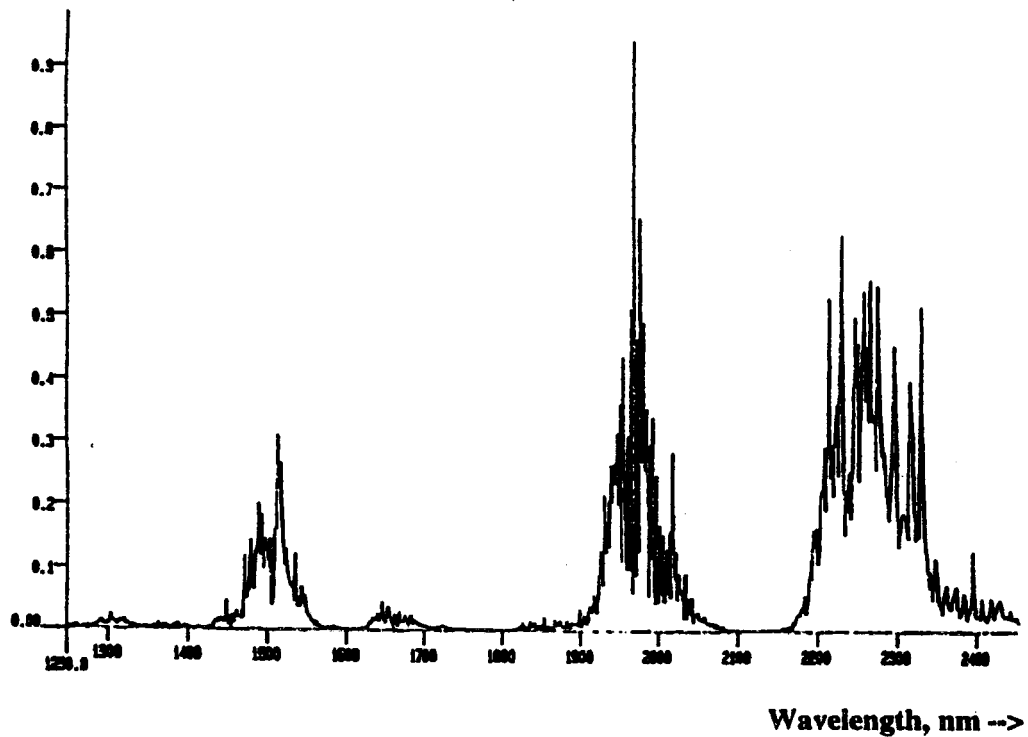


Figure 11 : Transmission spectrum of the reference/measurement test gas (ammonia and water vapour). This was measured in a Perkin-Elmer IR-Spectrometer (path length of 160 mm). The band at 1.505  $\mu\text{m}$  is caused by ammonia, and that at 1.92  $\mu\text{m}$  by water vapour.

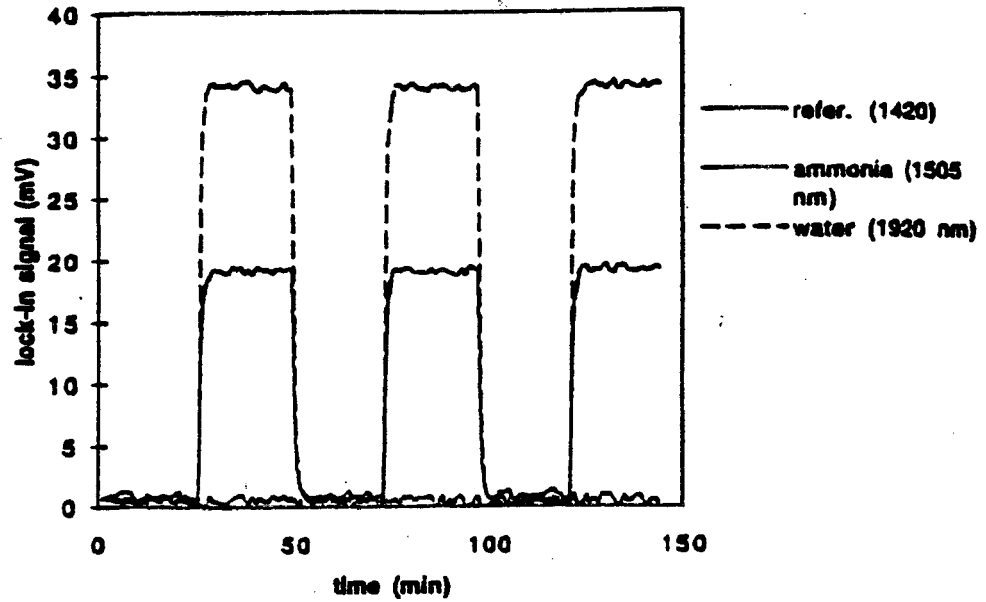


Figure 12 : Overlay of the measurements at the three wavelengths (1.505  $\mu\text{m}$ , 1.92  $\mu\text{m}$  and 1.42  $\mu\text{m}$ ) performed with the chopped-beam system of Figure 8.

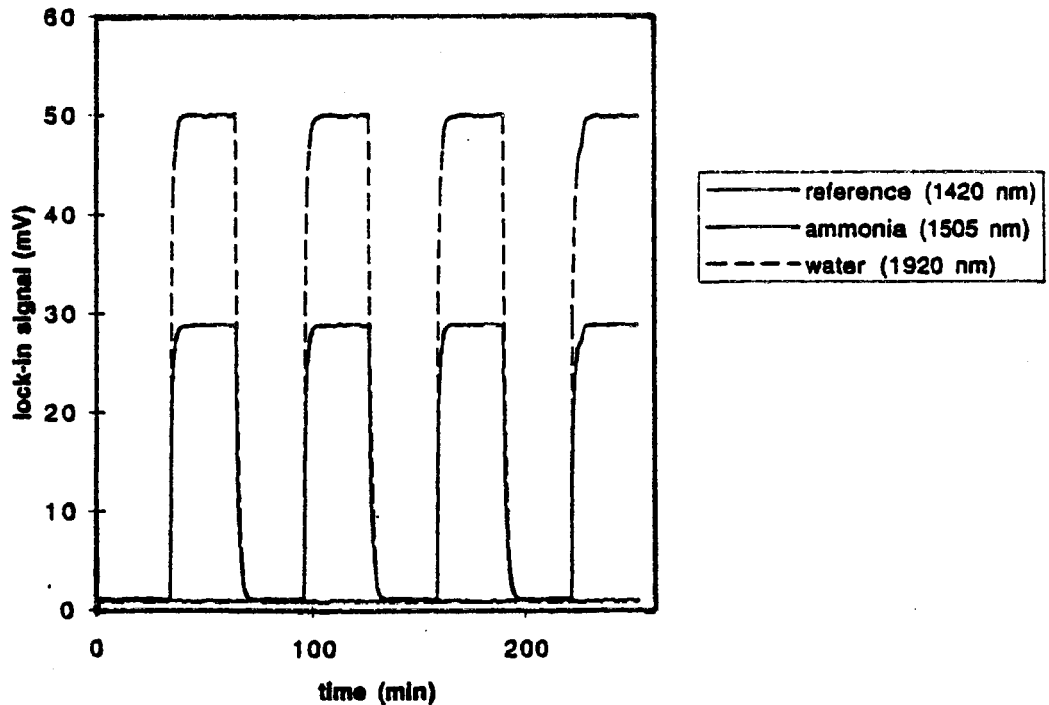


Figure 13 : Overlay of the measurements of the test gas at the three wavelengths (1.505, 1.92 and 1.42  $\mu\text{m}$ ), using the complementary-modulated source system of Figure 9. The measurement cell was filled alternately with sample gas, and pure nitrogen.